doi:10.14311/ppt.2026.1.37
Plasma Physics and Technology **13**(1):37–42, 2026

SPECTROSCOPIC DIAGNOSTICS OF ARC DISCHARGE PLASMA BETWEEN COMPOSITE Mo-Cu ELECTRODES WITH OXIDE IMPURITIES

A. Murmantsev*, A. Veklich, V. Apanasenko, A. Ivanisik

Faculty of Radiophysics, Electronics and Computer Systems, Taras Shevchenko National University of Kyiv, Volodymyrska str., 64/13, 01601, Kyiv, Ukraine

* murmantsev.aleksandr@gmail.com

Abstract. The work presents a comprehensive study of thermal plasma of electric arc discharge between composite electrodes of compositions Mo-50Cu-2Al_2O_3, Mo-50Cu-2Y_2O_3 and Mo-50Cu-5Y_2O_3 (in wt.%). The experiments were carried out in an argon flow at atmospheric pressure and a current of 3.5 A. A combination of spatially resolved synchronized optical emission spectroscopy and laser absorption spectroscopy methods was used to diagnose plasma parameters. The radial distributions of the excitation temperature and the number densities of copper and molybdenum atoms were determined using the Boltzmann plot technique. Based on the experimentally determined plasma parameters, the equilibrium plasma composition was calculated taking into account the dissociation and ionization products of oxide additives, in particular stable monoxides YO and AlO.

Keywords: Thermal plasma, arc discharge, composite electrodes, optical emission spectroscopy, laser absorption spectroscopy, oxide impurities.

1. Introduction

The development of modern energy, aerospace, and microelectronics is inextricably linked to the search for and implementation of new materials for electrical contacts capable of operating in extreme conditions of high currents, temperatures, and intense arc discharge. Among the large number of composite materials, researchers are particularly interested in systems based on copper and refractory metals, in particular molybdenum (Mo-Cu) [1, 2]. These materials, classified as pseudoalloys, combine a unique combination of properties: high electrical and thermal conductivity of copper with a high melting point, low coefficient of thermal expansion, and mechanical strength of molybdenum [2, 3]. Due to their high ablation resistance, these materials are also used in the manufacture of rocket engine nozzles and parts operating in high-speed, high-temperature gas flows [1]. In such critical modes, copper plays the role of a "transpiration cooler": it melts and evaporates, absorbing excess heat and creating a protective vapor curtain on the surface of the molybdenum frame [1].

However, increasing the requirements for the reliability of switching equipment requires further modification of these composites by introducing special oxide additives, such as aluminum oxide (Al_2O_3) and yttrium oxide (Y_2O_3) [4, 5]. The addition of Al_2O_3 provides dispersion strengthening and maintains grain boundary stability up to 900°C, while increasing melt viscosity to minimize copper spattering during arc discharge [4]. In turn, Y_2O_3 facilitates structural refinement and improves the wettability of the molybdenum skeleton, ensuring melt retention within capillaries and reducing erosion. The high melting point (2683 K) and chemical stability of Y_2O_3 provide enhanced durability under cyclic thermal stress [4–6].

A deep understanding of the processes of interaction of such a multicomponent plasma with the working surface requires the use of precision diagnostic methods, such as optical emission spectroscopy (OES) and laser absorption spectroscopy (LAS) [7]. These methods allow obtaining spatial distributions of temperature and atomic number density, which is critically important for analyzing the erosion behavior of composites.

The aim of this work is a comprehensive study of the behavior of Mo-Cu composite materials with impurities of Y_2O_3 and Al_2O_3 oxides under the thermal action of arc discharge plasma. Specifically, this study focuses on calculating the plasma composition and the total metal vapor content to provide a physical interpretation of the spectroscopic characteristics observed in the plasma between each electrode type. This approach allows for a detailed analysis of the influence of oxide impurities on the thermodynamic processes and the transition between different erosion mechanisms.

2. Experimental Investigation

The object of the investigation is the thermal plasma of an electric arc discharge burning in an argon flow at atmospheric pressure. The direct current in this series of experiments was maintained at 3.5 A, and the discharge gap was 8 mm. The electrodes are made in the form of rectangular rods with a square cross-section of 4×4 mm. Three types of composite materials based on a copper-molybdenum matrix with different additives, namely Mo-50Cu-2Al_2O_3 (in wt.%), Mo-50Cu-2Y_2O_3, Mo-50Cu-5Y_2O_3 are compared under thermal effect of arc discharge. The emission spectra were recorded from the middle cross-section of the discharge column,

which makes it possible to study the spatial distribution of parameters of the positive plasma column.

The recording the emission spectra began 15 seconds after the discharge ignition. This time interval was chosen to ensure the thermal stability of the plasma column due to the establishment of a quasi-stationary temperature regime of the electrodes. At the same time, this duration was insufficient for significant erosion wear or melting of the end surfaces of the electrodes, which allowed maintaining a constant value of the discharge gap and ensuring the identity and reproducibility of the experimental conditions for all types of composite materials studied.

For a comprehensive study of plasma parameters, a synchronized combination of optical emission spectroscopy (OES) and laser absorption spectroscopy (LAS) methods was used according to the experimental scheme shown in [7]. The synchronization accuracy between the OES and LAS measurements was maintained at 1 ms. The optical system was pre-calibrated using reference radiation sources to measure absolute intensity value in the spectral range of 430-650 nm [8], which maintained for each series of measurements. The spectral resolution of the spectrometer was 0.11 nm, while the spatial resolution was 0.015 mm.

The following spectral lines were identified in the emission spectra and were used to determine the excitation temperature of copper and molybdenum atoms population by Boltzmann plot technique [9]:

- Cu I 510.5, 515.3, 521.8, 570.0, 578.2 nm;
- Mo I 457.6, 461.0, 466.3, 467.2, 470.7, 473.1, 476.0, 481.9, 483.1, 486.8, 495.1, 495.8, 497.9, 536.1, 550.7, 553.3, 557.0, 563.2, 565.0, 568.9, 572.3, 575.1, 579.2, 585.8, 588.8, 603.1 nm.

Special attention was paid to the effect of self-absorption of molybdenum lines. According to previous studies [10], the Mo I 550.7, 553.3, 557.0 and 603.1 nm exhibit a significant degree of self-absorption (from 45% to 86%). Therefore, these lines were excluded from further determination of plasma parameters to avoid systematic errors.

Local values of the emission intensity $\epsilon(r)$ were calculated from the chordal observables $I(x)$ by solving the Abel integral equation by the Bockasten method at 10 points [11], assuming axial symmetry of the discharge [9].

For additional validation of the obtained temperatures, the data determined by the LAS method were incorporated into the Boltzmann plot technique. In particular, the approach described in [7] was used, which utilize both data obtained from the OES and from the LAS (see eq.(6) in [7]). A typical Boltzmann plot, determined at a distance of 2.17 mm from the axis of the arc discharge taking into account both the OES data (population density of the upper levels of the corresponding spectral lines) and the LAS

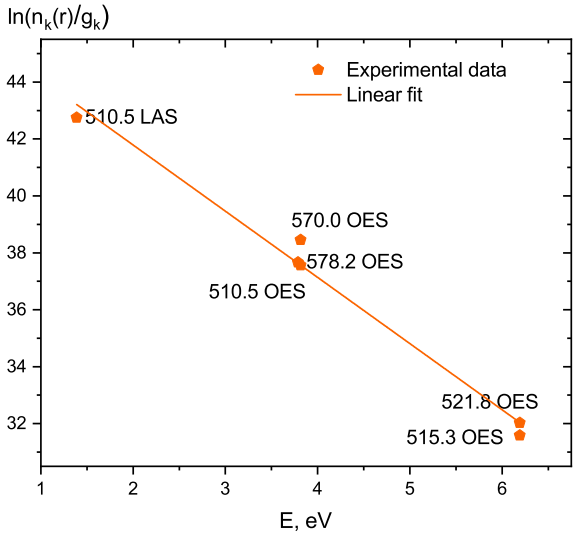

Figure 1. Typical Boltzmann plot based on the obtained population densities by synchronized LAS and OES (radial distance from arc axis r = 2.17 mm)

data (population of the lower energy level of the Cu I 510.5 nm spectral line [7]), is presented in Fig.1.

3. Results and Discussions

The excitation temperatures of copper and molybdenum atoms for each type of discharge, determined by the Boltzmann plot technique based on the absolute intensities of the Cu I, Mo I spectral lines and including both LAS and OES data, are shown in Fig.2 (black squares, red circles, and blue triangles, respectively).

One can see that for the plasma of electric arc discharges between the composite materials Mo-50Cu-2Al_2O_3 and Mo-50Cu-2Y_2O_3, the temperatures determined independently based on the Cu I and Mo I spectral lines coincide within the experimental error (~5%) along the entire radius. However, for the composite with an admixture of 5% Y_2O_3, a discrepancy of these temperatures is observed.

It can be seen that for the case of electrodes with 2% Y_2O_3 and Al_2O_3, the excitation temperatures obtained from the OES and from the OES combined with the LAS coincide. In the case of electrodes with 5% Y_2O_3, the temperature determined based on the Cu I spectral lines increases and begins to coincide within the error with the temperature determined based on the Mo I spectral lines. The reason for the initial mismatch of the radial temperature distributions determined from a different set of spectral lines may be the presence of self-absorption of the copper spectral lines.

To confirm this assumption, the degree of self-absorption of the Cu I 510.5 nm line was estimated for each of the modes, similarly to the work [7]. Indeed, for the case of 5% Y_2O_3, this degree can reach 35%, which affects the further determination of the temperature. Since the LAS method does not require considering self-absorption [12], taking into account

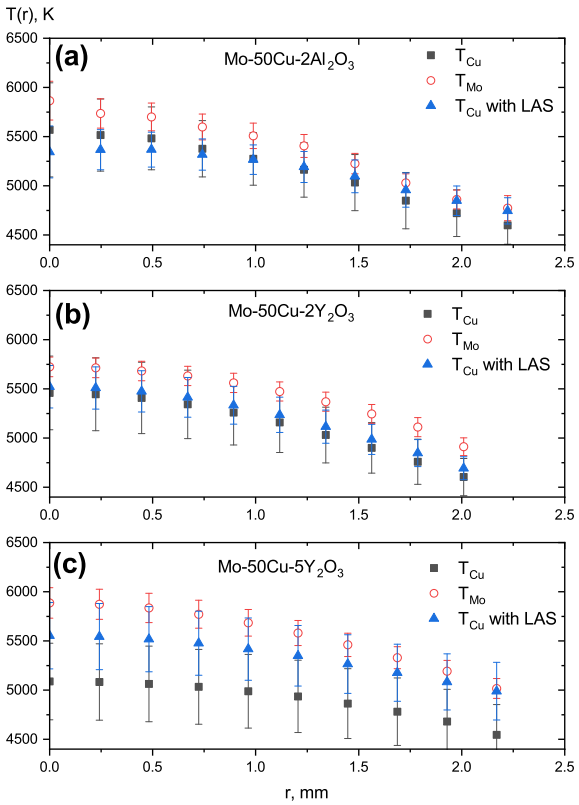

Figure 2. Radial distributions of excitation temperatures obtained by Boltzmann plot technique based on the emission intensities of both Cu I (black squares), Mo I (red circles) spectral lines, and with both LAS and OES data (blue triangles) in plasma of arc discharge between (a) Mo-50Cu-2Al$_2$O$_3$, (b) Mo-50Cu-2Y$_2$O$_3$, and (c) Mo-50Cu-5Y$_2$O$_3$ composite electrodes

the data obtained from LAS makes it possible to neglect the influence of this effect and to obtain more valid data for determining both the temperature and number densities of copper atoms.

Temperature values determined from the Mo I spectral lines tend to be slightly higher in all cases, particularly on the discharge axis, while converging with T_{Cu} at the periphery. This discrepancy can be attributed to several factors. First, the range of upper energy levels available for Mo I on the Boltzmann plot is significantly narrower (~2 eV) compared to the range for Cu I (~4.2 eV), which increases the sensitivity of the temperature determination to experimental uncertainties. The error bars for the excitation temperatures were derived from the standard deviation of the linear fitting on the Boltzmann plots. Second, although Mo I lines with significant self-absorption were excluded from the analysis, residual self-absorption may still affect other lines, potentially leading to an overestimation of the temperature. Overall, the temperature profiles for all three discharge modes do not differ significantly within the error bars (~5%), indicating that metal vapors are the primary species sustaining the arc discharge. This suggests that oxide additives do not have a decisive influence on the formation of the plasma channel under these conditions.

Based on the obtained experimental values of $T(r)$ and $n(r)$, the equilibrium plasma composition was calculated [13]. The radial distribution of temperature determined from the Cu I spectral lines (incorporating LAS data) was used as the primary input parameter for the plasma composition calculations. Consequently, the radial distribution of the molybdenum atom number density was recalculated based on this specific temperature profile and the absolute emission intensity of the Mo I 585.8 nm spectral line, following the Boltzmann distribution law as described in [9]. Unlike the simplified models used in [9], in this work the impurities (Al_2O_3 and Y_2O_3) were taken into account. In particular, the equation for the dissociation of YO (AlO) and O_2 molecules, the Saha equations for the ionization of Y (Al) atoms and YO (AlO) molecules were added to the system. It is suggested that molecules Y_2O_3 (Al_2O_3), as well as intermediate products such as YO_2 (AlO_2), YO_3 (AlO_3), Y_2O (Al_2O) etc. instantly dissociate in the high-temperature zone of the plasma and their concentration is negligibly small [14]. At the same time, YO and AlO monoxides are sufficiently thermally stable compounds to remain in the gas phase even at the high temperatures of the plasma column. In addition, it was assumed that YO^+ ions can make a significant contribution to the conductivity of the plasma due to their relatively low ionization potential (6.11 eV).

To ensure closure of the system of equations for equilibrium plasma composition, additional stoichiometric constraints were incorporated. These include mass balance equations stipulating the Y(Al) to O atomic ratio, as well as the relative concentration of the metal matrix to oxide impurities (2% and 5% by weight) according to the initial electrode composition.

The partition functions for YO molecules and YO^+ ions are taken from [15], while those for AlO molecules and AlO^+ ions are taken from [16, 17].

Radial distributions of the equilibrium plasma composition for each of the studied discharge types are presented in Fig.3. The plasma composition contains experimentally determined radial distributions of number densities of copper n_{Cu} and molybdenum atoms n_{Mo}, which include the calculated electron density n_e, number densities of neutral atoms n_{Ar}, ions n_{Ar^+}, n_{Cu^+}, n_{Mo^+}, atoms and ions of additives n_Y (n_{Al}), n_{Y^+} (n_{Al^+}), as well as the products of dissociation and ionization of oxygen and monoxides: n_O, n_{O^+}, n_{O_2}, n_{YO} (n_{AlO}) and n_{YO^+} (n_{AlO^+}).

One can see that the electron density, which determines the total electrical conductivity of the plasma, remains stable for each studied modes and varies within the range of $3.6 \cdot 10^{20}$ to $5.2 \cdot 10^{20}$ m^{-3}. In the cases of 2% Al_2O_3 and 2% Y_2O_3, the decisive contribution to the plasma conductivity is provided by the thermal ionization of molybdenum. Such a dominant role is due to the significantly lower ionization potential of molybdenum (7.09 eV) compared to copper

(7.73 eV) [9]. However, for the mode with 5% Y_2O_3, the contributions of copper and molybdenum become comparable, and the number densities of Cu^+ and Mo^+ ions practically coincide. This is explained by a significant increase in the total number density of copper atoms in the plasma when using composites with a high content of yttrium oxide, which compensates for the difference in ionization potentials.

The contribution of ionization of additive atoms to the total electron balance has a pronounced radial dependence. In the case of an aluminum impurity (2% Al_2O_3), its share is approximately 4.5% at the axis of the discharge, increasing to 7.7% at its periphery. For 2% Y_2O_3, the contribution of yttrium is about 3% at the arc axis with a further increase to 6.5% at the periphery of the plasma column. The more significant contribution of aluminum compared to yttrium is due to two factors: first, its lower ionization potential (5.99 eV versus 6.22 eV for yttrium); secondly, a significantly higher total number density of aluminum atoms in the gas phase (n_{Al} is an order of magnitude higher than n_Y). The latter is associated with a lower thermal stability of AlO molecules compared to YO, which leads to their faster dissociation and a more intensive supply of free metal atoms to the plasma.

A characteristic feature of the discharge with 5% Y_2O_3 is the stability of the yttrium contribution to ionization (about 1%) along the entire studied radius. Such uniformity correlates with a smaller radial temperature gradient in this type of discharge (see Fig.2, c), which ensures a homogeneous distribution of both the processes of dissociation of oxide compounds and the subsequent ionization of impurity atoms. The increase in the percentage contribution of the additives (Al and Y) at the periphery in other modes is explained by the fact that their ionization potentials are significantly lower than the corresponding values for copper and even molybdenum, which makes them critically important for maintaining conductivity in the colder regions of the plasma.

Analysis of the molecular composition showed that the number density of AlO^+ ions is three orders of magnitude lower than the number density of YO^+ molecular ions. This discrepancy is directly related to the energy advantage of ionization of yttrium monoxide, the ionization potential of which is 6.1 eV, while for AlO this value reaches 9.53 eV. Nevertheless, the number densities of both types of molecular ions remain insignificant in the overall plasma balance.

The radial distributions of the metal vapors contents (X_{Cu} and X_{Mo}) in the plasma are shown in Fig.4. It is worth noting that the calculated content of oxide impurity vapors is not presented in the graphs, since its value in each modes does not exceed $7 \cdot 10^{-5}$%.The following equation was used to calculate vapor contents:

$$X_j(r) = \frac{n_j(r) + n_j^+(r)}{\Sigma n_i(r)} * 100\% \qquad (1)$$

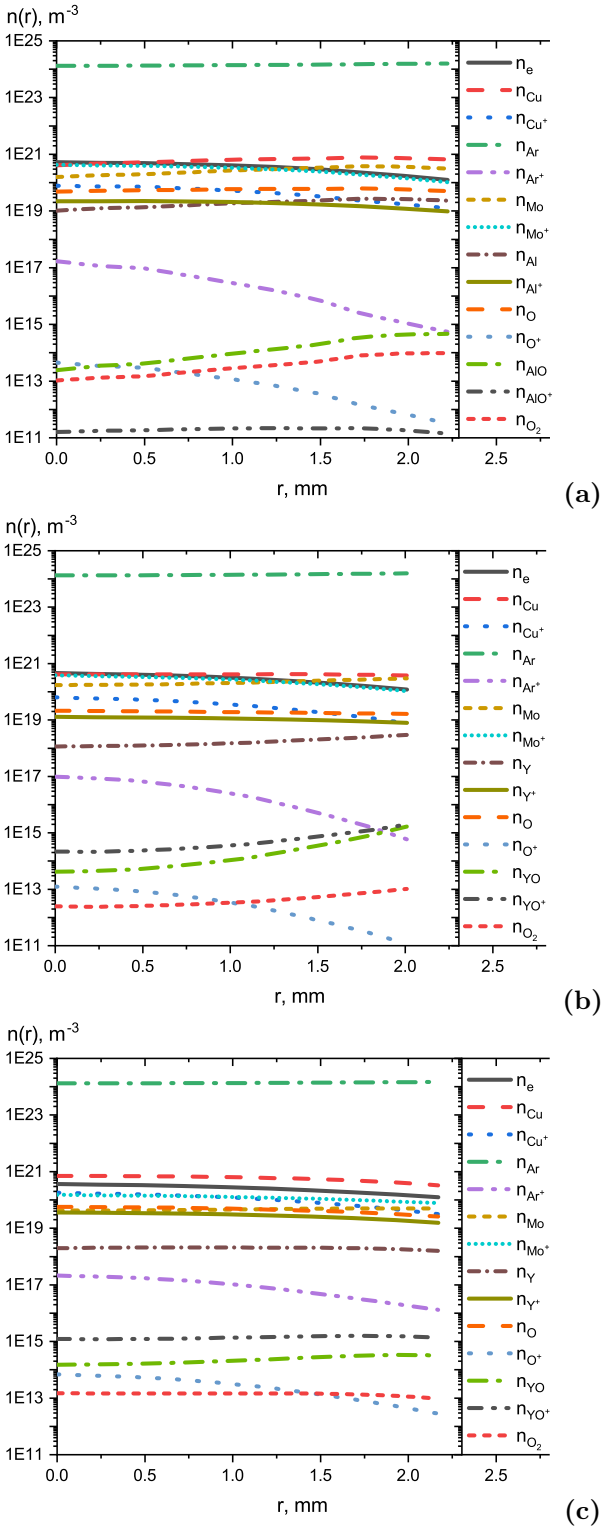

Figure 3. Radial distributions of equilibrium plasma compositions of arc discharge between (a) Mo-50Cu-2Al_2O_3, (b) Mo-50Cu-2Y_2O_3, and (c) Mo-50Cu-5Y_2O_3 composite electrodes

where the index j corresponds to copper, molybdenum or total impurity (Al_2O_3 or Y_2O_3). In the case of complex impurities, the total number density of neutral particles was considered as the sum $n_j = n_{Y(Al)} + n_{YO(AlO)} + n_O + n_{O_2}$, and $n_j^+ =$

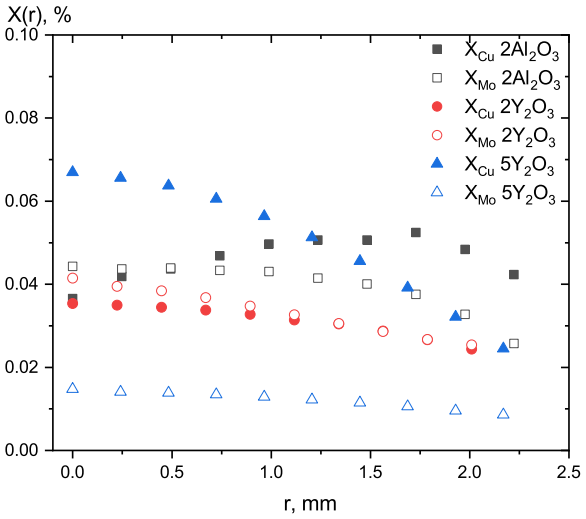

Figure 4. Radial distributions of metal vapors contents in arc discharge between Mo-50Cu-2Al_2O_3 (black squares), Mo-50Cu-2Y_2O_3 (red circles), and Mo-50Cu-5Y_2O_3 (blue triangles) composite electrodes

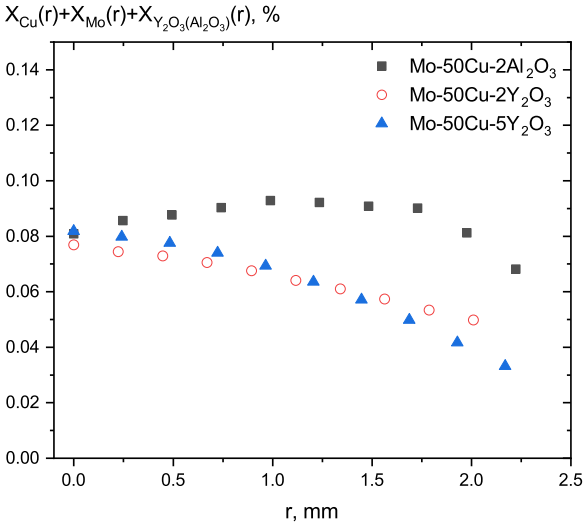

Figure 5. Radial distributions of total vapor content of electrodes origin elements in the plasma of arc discharge between each type of composite electrodes

$n_{Y^+(Al^+)} + n_{YO^+(AlO^+)} + n_{O^+}$ for ionized components. The denominator Σn_i corresponds to the total number density of all heavy particles of the plasma in the approximation of local thermodynamic equilibrium.

One can see that in the plasma between the composite electrodes Mo-50Cu-2Al_2O_3 and Mo-50Cu-2Y_2O_3 the content of copper and molybdenum vapors remains approximately the same along the entire investigated radius. This behavior indicates a relatively uniform evaporation of the matrix components. However, in the case of a discharge between Mo-50Cu-5Y_2O_3 electrodes, a qualitatively different picture is observed: the content of copper vapors on the discharge axis is approximately 4.5 times higher than the content of molybdenum, and also twice as high as the concentration of copper in the plasma of other studied modes. This effect may indicate a fundamental change in the erosion mechanism: from stationary evaporation of components to selective "sweating" and intensive destruction of the copper matrix from the refractory molybdenum skeleton [18].

The physical reason for such a transformation is the specific effect of yttrium oxide on thermodynamic processes in the surface layer of the electrode. Y_2O_3 is characterized by a high melting point (2683 K) and significantly lower thermal conductivity compared to copper and even molybdenum. Oxide particles are able to form cluster structures or almost continuous thermal insulating layers that prevent effective heat removal from the working surface into the electrode. This leads to significant local overheating of the surface areas of the copper phase with a relatively low boiling point (2735 K). As a result, intensive evaporation of copper occurs, while the more refractory molybdenum skeleton (melting point 2896 K) retains structural stability. In addition, the massive flow of copper vapor creates the effect of partial shielding of the molybdenum surface from the direct thermal effect of the plasma, which further explains the decrease in its relative concentration in the discharge.

When comparing the total content of elements of electrode origin, which was calculated as the total fraction of copper, molybdenum and the corresponding oxide additive ($X_{Cu} + X_{Mo} + X_{Y_2O_3(Al_2O_3)}$), no significant quantitative difference was found between the studied discharge types (see Fig.5). Such stability of the total yield of the substance indicates that the variation of the impurities considered in this work does not have a crucial effect on the overall erosion resistance of materials at given discharge parameters. However, it is worth emphasizing that an increase in the concentration of yttrium oxide significantly changes the nature of the erosion processes. A comparison with previous results involving different electrode stoichiometries, such as Mo-25Cu and Mo-75Cu, indicates that the addition of oxide impurities does not significantly impact the overall erosion resistance. In terms of total metal vapor content, the Mo-75Cu composite remains the most optimal configuration, which is primarily attributed to its superior thermal conductivity [9].

4. Conclusions

A comprehensive study of the thermal plasma of an electric arc discharge between Mo-50Cu-2Al_2O_3, Mo-50Cu-2Y_2O_3 and Mo-50Cu-5Y_2O_3 (in wt.%) composite electrodes was conducted. The experiments were carried out in an argon flow at atmospheric pressure and a current of 3.5 A.

The use of a synchronized combination of OES and LAS methods allowed for precise diagnostics of plasma parameters. The LTE can be realized for each studied modes, which indicated by the coincidence of the excitation temperatures of the energy levels of copper and molybdenum atoms, determined by the

Boltzmann plot technique.

It was found that aluminum and yttrium impurities play an important role in maintaining the ionization balance at the periphery of the discharge, where their contribution increases to 6.5–7.7%. The greater efficiency of aluminum compared to yttrium is due to the more intense dissociation of AlO molecules and the lower ionization potential of Al atoms. Despite the low ionization potential of the YO molecule (6.1 eV), the number density of molecular ions remains insignificant in the overall composition of the plasma.

In summary variation of oxide additives within 2–5% does not significantly change the total vapor content of electrode materials, which indicates a similar erosion resistance of the studied materials. However, increasing the concentration of Y_2O_3 to 5% can transform the erosion mechanism: due to the low thermal conductivity of oxide clusters, local overheating of the surface occurs, which causes selective evaporation of the copper matrix while maintaining the stability of the molybdenum skeleton.

5. Acknowledgments

This work was supported by the National Research Foundation of Ukraine (Grant № 2023.03/0169).

The authors express their gratitude to Mr. Mykhailo Papizh, and Ms. Daryna Sych for their assistance in the organization of this experimental research and data processing.

In addition, the authors are grateful to Dr. Oleksandr Tolochyn from the Frantsevich Institute for Problems of Materials Science NAS of Ukraine for the materials provided under the cooperation agreement.

References

[1] J. Cai, Q. Jiang, K. Feng, and H. Zhou. Tailoring microstructure and properties of W-Mo-Cu composites fabricated via infiltration sintering: Effects of graphene addition and skeleton relative density. *Materials*, 18(11):2539, 2025. doi:10.3390/ma18112539.

[2] H. Zhang and G.-H. Zhang. Influence of Ti addition on the microstructure and comprehensive properties of Mo-Cu alloy. *Journal of Materials Research and Technology*, 30:2833–2847, 2024. doi:10.1016/j.jmrt.2024.04.050.

[3] P. A. Benavides, B. Soto, and R. H. Palma. Liquid phase sintering of mechanically alloyed Mo-Cu powders. *Materials Science & Engineering A*, 701:237–244, 2017. doi:10.1016/j.msea.2017.06.090.

[4] Y. Li, M. Zhou, Y. Zhang, et al. Effect of Y2O3 on the electrical contact behavior of Al2O3-Cu/MoTa composites. *Coatings*, 13(2):252, 2023. doi:10.3390/coatings13020252.

[5] X. Zheng, M. Zhou, Y. Zhang, et al. Microstructure and electrical contact behavior of Al2O3-Cu/30W3SiC(0.5Y2O3) composites. *Journal of Materials Research and Technology*, 22:2158–2173, 2023. doi:10.1016/j.jmrt.2022.12.071.

[6] Z. Ma, M. Zhou, B. Tian, et al. Nano- Y2O3 effects on the electrical contact properties of Al2O3-Cu/35Cr3TiB2 composites. *Materials Characterization*, 207:113474, 2024. doi:10.1016/j.matchar.2023.113474.

[7] A. Murmantsev, A. Veklich, V. Apanasenko, et al. Synchronized laser absorption and optical emission spectroscopy of plasma with copper vapour admixtures. *Problems of Atomic Science and Technology*, 155(1):123–128, 2025. doi:10.46813/2025-155-123.

[8] A. Murmantsev. Investigation of spatial distribution of metal vapours admixtures in the plasma of an electric arc discharge. *Problems of Atomic Science and Technology*, 146(4):139–146, 2023. doi:10.46813/2023-146-139.

[9] A. Veklich, A. Murmantsev, V. Apanasenko, and O. Tolochyn. Spectroscopy of plasma of electric arc discharge between Cu-Mo composite electrodes. *Plasma Physics and Technology*, 12(1):73–78, 2025. doi:10.14311/ppt.2025.1.73.

[10] A. Murmantsev, A. Veklich, D. Sych, et al. Peculiarities of spectroscopy of thermal plasma with copper and molybdenum vapour admixtures. *Plasma Physics and Technology*, 12(1):67–72, 2025. doi:10.14311/ppt.2025.1.67.

[11] K. Bockasten. Transformation of observed radiances into radial distribution of the emission of a plasma. *Journal of the Optical Society of America*, 51(9):943–947, 1961. doi:10.1364/JOSA.51.000943.

[12] S. Reuter, J. S. Sousa, G. D. Stancu, and J.-P. H. van Helden. Review on VUV to MIR absorption spectroscopy of atmospheric pressure plasma jets. *Plasma Sources Science and Technology*, 24(5):054001, 2015. doi:10.1088/0963-0252/24/5/054001.

[13] A. Veklich, A. Lebid, R. Minakova, et al. Peculiarities of interaction of electric arc plasma and composite electrodes' working surface. In *Proceedings of the 21st Symposium on Physics of Switching Arc (FSO 2015)*, 2015. Conference Paper.

[14] P. Andre, M. Abbaoui, A. Augeard, et al. Study of condensed phases, of vaporization temperatures of aluminum oxide and aluminum, of sublimation temperature of aluminum nitride and composition in an air aluminum plasma. *Plasma Chemistry and Plasma Processing*, 36:1161–1175, 2016. doi:10.1007/s11090-016-9704-7.

[15] L. V. Gurvich, I. V. Veyts, and C. B. Alcock. *Thermodynamics Properties of Individual Substances*. Hemisphere Publishing Corp., New York, 4th edition, 1989. Vols. 1–3.

[16] T. Bai, Z. Qin, and L. Liu. Ultraviolet spectroscopy of AlO from first principle. *Journal of Quantitative Spectroscopy & Radiative Transfer*, 302:108587, 2023. doi:10.1016/j.jqsrt.2023.108587.

[17] J. Chase, M. W. NIST-JANAF thermochemical tables. *Journal of Physical and Chemical Reference Data*, Monograph 9:1–1951, 1998. doi:10.18434/T42S31.

[18] A. Veklich, S. Fesenko, and V. Boretskij. Plasma pecularities of arc discharge between carbon-copper electrodes. *Plasma Physics and Technology*, 6(2):152–155, 2019. doi:10.14311/ppt.2019.2.152.